

Complex Modal Testing of Asymmetric Rotors Using Magnetic Exciter Equipped with Hall Sensors

Chong-Won Lee*

Center for Noise and Vibration Control, KAIST, Taejon 305-701, Korea

Si-Kyoung Kim

Advanced Engineering Center, Samsung SDI, Kyunggi-do 442-391, Korea

The complex modal testing methods developed for asymmetric rotors are briefly discussed and their performances are experimentally evaluated. For the experiments, a laboratory test rotor is excited by using a newly developed, cost effective magnetic exciter equipped with Hall sensors, which measure the excitation forces. It is concluded that the exciter system is characterized by a wide bandwidth and a high resolution for both the excitation and force measurement, and that the one-exciter/two-sensor technique for complex modal testing of asymmetric rotors is superior to the standard two-exciter/two-sensor technique in terms of practicality and realization.

Key Words : Complex Modal Testing, dFRFs, Asymmetric Rotors, Magnetic Exciter, Hall Sensors

Nomenclature			
F	: Magnetic force	k	: Stiffness of simple rotor
f_y, f_z	: y- and z- direction force vectors	$\mathbf{p}, \bar{\mathbf{p}}$: Complex displacement vectors in stationary coordinate
$\mathbf{g}, \bar{\mathbf{g}}, \tilde{\mathbf{g}}$: Complex force vectors in stationary coordinate	$P(j\omega), \hat{P}(j\omega)$: Fourier transforms of \mathbf{p} and $\bar{\mathbf{p}}$
g	: Air gap	$S_{ik}, i,k=p,g,\bar{g},\tilde{g}$: Directional auto- and cross- spectral density functions
$G(j\omega), \hat{G}(j\omega), \tilde{G}(j\omega)$: Fourier transforms of $\mathbf{g}, \bar{\mathbf{g}}$ and $\tilde{\mathbf{g}}$	y,z	: y- and z- directional displacement vectors
$H_{g\bar{p}}, H_{\bar{g}p}, H_{\tilde{g}p}$: Normal dFRFs	$\gamma_{g\bar{g}}^2 (\gamma_{\tilde{g}\tilde{g}}^2)$: Directional coherence function between $\mathbf{g}, \bar{\mathbf{g}}$ ($\mathbf{g}, \tilde{\mathbf{g}}$)
$H_{\bar{g}p}, H_{\tilde{g}p}$: Reverse dFRFs of anisotropic rotors	Ω	: Rotational speed
$H_{\tilde{g}p}, H_{g\bar{p}}$: Reverse dFRFs of asymmetric rotors	$F(\bar{F})$: Forward (conjugate forward) mode
$\hat{H}_{ik}, i,k=p,g,\bar{g},\tilde{g}$: Estimated dFRFs using unidirectional excitation	$B(\bar{B})$: Backward (conjugate backward) mode
j	: Imaginary number = $\sqrt{-1}$		

* Corresponding Author,
E-mail : cwlee@novic.kaist.ac.kr
TEL : +82-42-869-3016 ; **FAX :** +82-42-869-8220
 Center for Noise and Vibration Control, Department of Mechanical Engineering, KAIST, Science Town, Taejon 305-701, Korea. (Manuscript Received September 26, 2000; Revised April 2, 2001)

1. Introduction

Nowadays, the operation of the rotating machinery involves high force and energy levels along with high operating speed so that failures in the rotating machines can often lead to severe

damage not only to the machines, but also to the surrounding equipments. The accidental or intended presence of asymmetry (rotating asymmetry) in a rotor system, which may be caused by the rotating machine failures, may significantly alter its dynamic characteristics, such as the unbalance response, critical speeds and stability, from those of the ideal isotropic (symmetric) rotor (Jei and Lee, 1988). Thus, the complex modal testing theories and methods have been extensively developed to accurately identify the asymmetric properties and understand the dynamic behavior of practical rotors (Lee, 1991; Lee, 1993). However, they all utilize the directional frequency response functions (dFRFs) defined on the basis of the complex inputs and outputs. Therefore, the new excitation and measurement techniques, which differ from the conventional ones, are required.

Lee and Kim (1992) developed a bi-directional magnetic exciter, equipped with a piezo-electric load cell, for the complex modal testing of anisotropic rotors (Lee and Kim, 1992). Since then, the magnetic exciters have been widely adopted for modal parameter identification of rotors. On the other hand, Gähler (1994) successfully adopted Hall sensors as a force transducer in a magnetic bearing system (Gähler and Forch, 1994).

In the early works by Joh and Lee (1996) for identification of the rotating asymmetry, a rotating coordinate system has been adopted to conveniently describe the equation of motion of asymmetric rotors (Joh and Lee, 1996). However, in the later works (Lee and Lee, 1997), it was found that it is much easier and more convenient to deal with the dFRFs in the stationary coordinate system than the rotating one, because the excitations and responses are usually measured with respect to the stationary coordinate system (Lee and Lee, 1997). Recently, Lee and Kwon (1999) also suggested that the modal testing method required for the identification of rotating asymmetry can be much simpler, requiring only a single exciter, compared to the case of the stationary asymmetry (anisotropy), which requires the standard bi-directional excitation method (Lee

and Kwon, 1999).

In this work, a cost effective magnetic exciter equipped with Hall sensors is developed for force measurement as well as the excitation of rotors. Preliminary force calibration experiments are performed to show that a Hall sensor can be used to measure the excitation force with good accuracy and relatively high bandwidth. Finally, the performances of the various modal testing methods developed for asymmetric rotors are experimentally evaluated with a laboratory test rotor and compared with respect to their implementation using the magnetic exciter equipped with Hall sensors.

2. Directional Frequency Response Functions

In general, a rotor-bearing system consists of the rotor and stator parts. Depending on the non-axisymmetric properties of the rotor and stator, a rotor-bearing system may be classified as follows (Joh and Lee, 1996): *isotropic (symmetric) rotor system*—both the rotor and the stator are axisymmetric; *anisotropic rotor system*—the rotor is axisymmetric but the stator is not; *asymmetric rotor system*—the stator is axisymmetric but the rotor is not; *general rotor system*—neither the rotor nor the stator is axisymmetric.

Using the stationary coordinate system, or XYZ, as shown in Fig. 1, the $N \times 1$ complex response and input vectors, $p(t)$ and $g(t)$, are

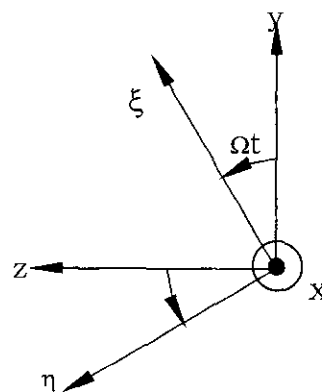


Fig. 1 Stationary (xyz) and rotating coordinate system

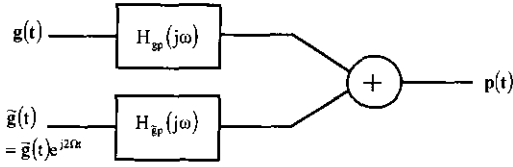


Fig. 2 Two complex inputs single complex output model for asymmetric rotor system

defined by the real response vectors, $y(t)$ and $z(t)$, and the real input vectors, $f_y(t)$ and $f_z(t)$, respectively, as

$$\begin{aligned} p(t) &= y(t) + jz(t), \quad \bar{p}(t) = y(t) - jz(t), \\ g(t) &= f_y(t) + jf_z(t), \quad \tilde{g}(t) = f_y(t) - jf_z(t) \end{aligned} \quad (1)$$

where j denotes the imaginary number, Ω is the rotational speed, and the bar denotes the complex conjugate.

For the asymmetric rotors, where the stator is axisymmetric but the rotor is not, the directional frequency response matrices (dFRMs) between the complex inputs and outputs are defined as (Joh and Lee, 1996; Lee and Lee, 1997)

$$\mathbf{P}(j\omega) = [\mathbf{H}_{gp}(j\omega) \quad \mathbf{H}_{\tilde{g}p}(j\omega)] \begin{bmatrix} \mathbf{G}(j\omega) \\ \tilde{\mathbf{G}}(j\omega) \end{bmatrix} \quad (2)$$

where $\mathbf{P}(j\omega)$, $\mathbf{G}(j\omega)$, $\tilde{\mathbf{G}}(j\omega)$ and $\tilde{\tilde{\mathbf{G}}}(j\omega) = \tilde{\mathbf{G}}\{j(\omega - 2\Omega)\}$ are the Fourier transforms of $p(t)$, $g(t)$, $\tilde{g}(t)$ and $\tilde{\tilde{g}}(t) = \tilde{g}(t)e^{j2\Omega t}$, respectively. Here $\mathbf{H}_{gp}(j\omega)$ is referred to as the *normal* dFRMs, whereas $\mathbf{H}_{\tilde{g}p}(j\omega)$ is referred to as the reverse dFRMs of the asymmetric rotor. Figure 2 shows the corresponding two complex inputs/single complex output model (Lee and Lee, 1997). The directional coherence function (dCOH) between $g(t)$ and $\tilde{g}(t)$, $\gamma_{\tilde{g}g}^2(j\omega)$, is defined, for the asymmetric rotor, as

$$\gamma_{\tilde{g}g}^2(j\omega) = \frac{|\mathbf{S}_{\tilde{g}g}(j\omega)|^2}{\mathbf{S}_{gg}(j\omega)\mathbf{S}_{\tilde{g}\tilde{g}}(j\omega)} \quad (3)$$

3. Modal Testing Methods for Asymmetric Rotors

3.1 One-exciter/two-sensor method

Lee and Lee (1996) showed that the input processes $g(t)$ and $\tilde{g}(t)$ for the asymmetric rotor should be individually stationary but may be jointly non-stationary for effective estimation of

dFRFs. On the other hand, since it normally holds that (Lee and Lee, 1997; Lee and Kwon, 1999; Bendat and Piersol, 1986)

$$\begin{aligned} \mathbf{S}_{\tilde{g}g}(j\omega, j\omega) &= \mathbf{T}\mathbf{S}_{\tilde{g}\tilde{g}}(j\omega) = 0, \text{ or} \\ \text{equivalently, } \gamma_{\tilde{g}g}^2(j\omega) &= 0 \end{aligned} \quad (4)$$

for a sufficiently long time record length, i. e., $T \gg \pi/2\Omega$, irrespective of the correlation between $g(t)$ and $\tilde{g}(t)$, the dFRFs can be estimated from (Lee and Lee, 1997; Lee and Kwon, 1999)

$$\mathbf{H}_{gp}(j\omega) = \frac{\mathbf{S}_{gp}(j\omega)}{\mathbf{S}_{gg}(j\omega)}, \quad \mathbf{H}_{\tilde{g}p}(j\omega) = \frac{\mathbf{S}_{\tilde{g}p}(j\omega)}{\mathbf{S}_{\tilde{g}\tilde{g}}(j\omega)} \quad (5)$$

Note that Eq. (5) is valid even when $g(t)$ and $\tilde{g}(t)$ are fully coherent. This implies that any unidirectional stationary random excitation in the y - z plane, necessitating only a single exciter, is sufficient for estimating the dFRFs of the asymmetric rotor systems. Therefore, it can be concluded that the estimation by the so-called one-exciter/two-sensor method is identical to that of the standard two-exciter/two-sensor method since Eq. (5) holds irrespective of the number of exciters (Lee and Lee, 1997).

3.2 Two-exciter/one-sensor method

The estimation methods for dFRFs of the asymmetric rotors are discussed when a unidirectional response measurement is available. The measured response, $y(t)$, of an asymmetric rotor along one direction, say the y -axis, can be written as

$$2y(t) = p(t) + \bar{p}(t) \quad (6)$$

Taking the Fourier transform of Eq. (6) and using Eq. (2), we obtain (Lee and Kwon, 1999)

$$\begin{aligned} 2\mathbf{Y}(j\omega) &= \mathbf{P}(j\omega) + \hat{\mathbf{P}}(j\omega) = \mathbf{H}_{gp}(j\omega)\mathbf{G}(j\omega) \\ &+ \mathbf{H}_{\tilde{g}p}(j\omega)\tilde{\mathbf{G}}(j\omega) + \mathbf{H}_{\tilde{g}p}(j\omega)\tilde{\tilde{\mathbf{G}}}(j\omega) \\ &+ \mathbf{H}_{\tilde{g}p}(j\omega)\tilde{\tilde{\mathbf{G}}}(j\omega) \end{aligned} \quad (7)$$

where $\mathbf{Y}(j\omega)$, $\mathbf{G}(j\omega)$, $\tilde{\mathbf{G}}(j\omega)$, $\hat{\mathbf{G}}(j\omega)$ and $\tilde{\tilde{\mathbf{G}}}(j\omega)$ are the Fourier transforms of $y(t)$, $g(t)$, $\tilde{g}(t)$, $\hat{g}(t)$ and $\tilde{\tilde{g}}(t) = g(t)e^{-j2\Omega t}$, respectively. Each random input process is stationary, but may be jointly non-stationary for estimating the dFRFs from the signals $g(t)$, $\tilde{g}(t)$, $\hat{g}(t)$, $\tilde{\tilde{g}}(t)$ and $p(t)$. For non-stationary random processes, the double frequency spectral density functions at any pair of

fixed frequencies, ω_1 and ω_2 , are defined by the expected values, and their relationships are derived for $\omega_1 = \omega_2 = \omega$, to estimate the dFRFs by (Lee and Kwon, 1999)

$$\begin{bmatrix} H_{gp}(j\omega) \\ H_{gp}(j\omega) \\ H_{gp}(j\omega) \\ H_{gp}(j\omega) \end{bmatrix} = \begin{bmatrix} S_{gg}(j\omega) & S_{g\hat{g}}(j\omega) & S_{g\hat{g}}(j\omega) \\ S_{\hat{g}\hat{g}}(j\omega) & S_{\hat{g}\hat{g}}(j\omega) & S_{\hat{g}\hat{g}}(j\omega) \\ S_{\hat{g}\hat{g}}(j\omega) & S_{\hat{g}\hat{g}}(j\omega) & S_{\hat{g}\hat{g}}(j\omega) \\ S_{\hat{g}\hat{g}}(j\omega) & S_{\hat{g}\hat{g}}(j\omega) & S_{\hat{g}\hat{g}}(j\omega) \end{bmatrix}^{-1} \begin{bmatrix} 2S_{gy}(j\omega) \\ 2S_{gy}(j\omega) \\ 2S_{gy}(j\omega) \\ 2S_{gy}(j\omega) \end{bmatrix} \quad (8)$$

For signals taken with a sufficiently long record length such that $T \gg \pi/2\Omega$, with $\Omega \neq 0$, Eq. (8) reduces to (Lee and Kwon, 1999)

$$\begin{aligned} H_{gp}(j\omega) &= 2 \frac{S_{gy}(j\omega)}{S_{gg}(j\omega)} \frac{1 - \frac{S_{gy}(j\omega)S_{g\hat{g}}(j\omega)}{S_{gy}(j\omega)S_{\hat{g}\hat{g}}(j\omega)}}{1 - \gamma_{g\hat{g}}^2(j\omega)} \\ &= 2 \frac{S_{gy}(j\omega)}{S_{gg}(j\omega)}, \\ \text{if } \gamma_{g\hat{g}}^2(j\omega) &= 0, H_{gp}(j\omega) = 2 \frac{S_{gy}(j\omega)}{S_{gg}(j\omega)} \end{aligned} \quad (9)$$

since

$$\begin{aligned} S_{g\hat{g}}(j\omega) &= S_{\hat{g}\hat{g}}(j\omega) = S_{\hat{g}\hat{g}}(j\omega) = S_{\hat{g}\hat{g}}(j\omega) \\ &= S_{\hat{g}\hat{g}}(j\omega) = 0 \end{aligned}$$

4. Magnetic Exciter Equipped with Hall Sensors

4.1 Design of magnetic exciter

The newly developed magnetic exciter consists

of four magnet cores and four Hall sensors (SIEMENS, KSY44). Each Hall sensor was placed between the magnet core and rotor to measure the magnetic flux density as shown in Fig. 3. The measured magnetic flux density was amplified and squared by a signal conditioner. The Hall sensors were calibrated with a reference force transducer so that the excitation forces can be measured indirectly via the Hall sensor outputs. Figure 4 depicts the operating principle of the magnetic exciter equipped with Hall sensors.

Assuming that the leakage of the magnetic flux is negligible, the magnetization curve is linear and furthermore the magnetic flux density is uniform across the poleface. Then the magnetic force, F ,

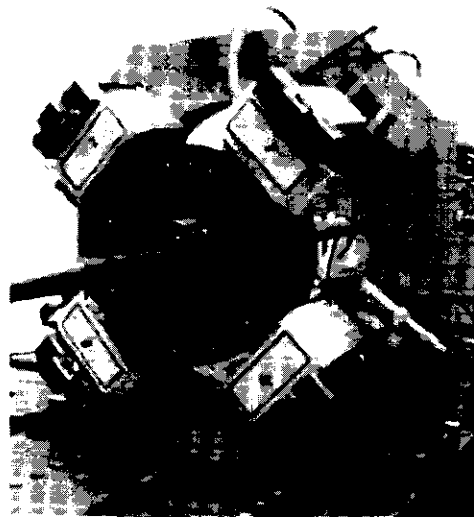


Fig. 3 Photo of magnetic exciter equipped with Hall sensors

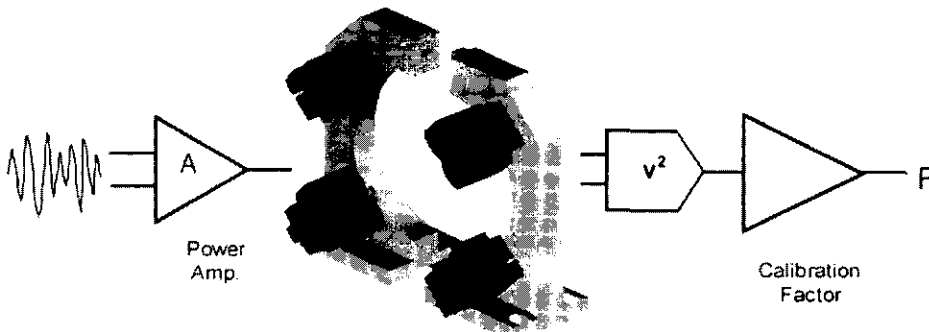


Fig. 4 Operation principle of magnetic exciter

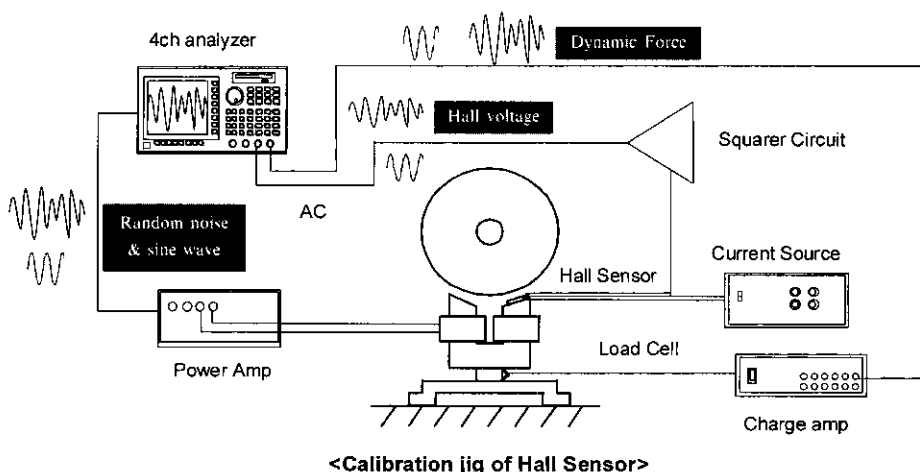


Fig. 5 Experimental set-up for the force calibration of Hall sensor

can be written in terms of the flux density, B , as Lee et al. (1997)

$$F = \frac{B^2 A}{\mu_0} = \frac{\mu_0 N^2 I^2 A}{4g^2} \quad (10)$$

where I is the current, A is the projected area of the curved poleface, N is the number of coil turns, g is the nominal air gap, and μ_0 is the permeability of free space ($=4 \times 10^{-7}$ H/m). The design parameters used for the magnetic exciter are: $N=305$ turns, $I=1$ A, $g=1.6$ mm, and $A=240$ mm².

The characteristics of the magnetic exciter equipped with Hall sensors are as follows: (1) It is cost effective and easy to install/assemble; (2) The diameter of the exciter can be adjusted so that it is possible to excite the rotor with various diameters ($\varnothing 75 \pm 10$ mm); (3) It has a wide frequency bandwidth; and (4) It is possible to excite the rotor at any location.

4.2 Calibration of hall sensor as a force transducer

The magnetic force is proportional to the Hall voltage squared, for the given pole face area, A , as given by

$$\frac{F}{B^2} = \frac{A}{\mu_0} = \text{const.} \quad (11)$$

The equation implies that the magnetic force along the magnetic poles can be computed from the corresponding measured flux density. Note that the calibration factor remains nearly un-

changed, irrespective of the change in air gap.

Figure 5 shows the experimental set-up for the Hall sensor calibration. It consists of a jig, a stationary rotor, a reference piezoelectric force transducer, a magnet core and a Hall sensor. The piezoelectric force transducer is placed between the jig and magnet core. The Hall sensor is placed on top of the pole face between the magnetic core and rotor. The current supplied from the power amplifier drives the magnetic core and the amplifying and squarer circuit amplifies the output voltage from the Hall sensor.

Two separate procedures are required to calibrate the Hall sensor. In the first procedure, a band-limited random excitation signal, which is generated by a 4-channel FFT analyzer (HP 35670A), is fed into the power amplifier for the magnetic core in order to excite the rotor. The force transducer and the Hall sensor signals are fed back to the FFT analyzer for data processing so that the frequency response functions (FRF's) between the force transducer signals and the Hall sensor signals can be estimated. Figure 6 shows that the frequency bandwidth (± 3 dB) is about 830 Hz. In the second procedure, a sinusoidal signal with 100 Hz, which is within the frequency bandwidth, is applied to the magnetic core in order to excite the rotor. The signal from the Hall sensor is amplified and squared by a signal conditioner. Then the output signals of the force transducer and the Hall sensor are measured simulta-

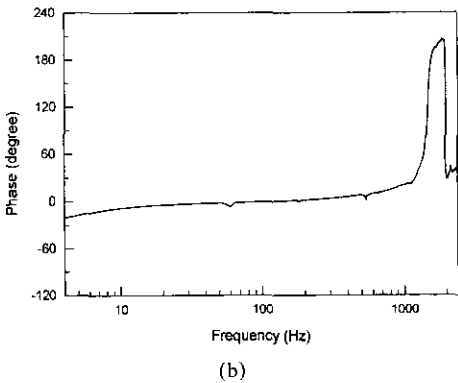
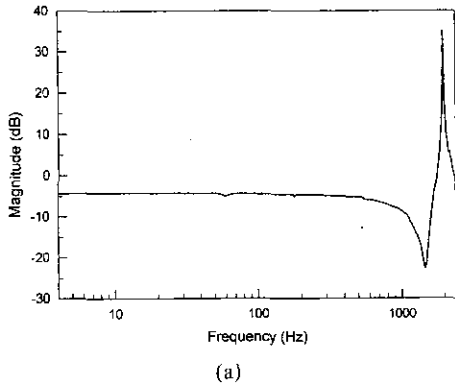


Fig. 6 Force calibration of Hall sensor: random test

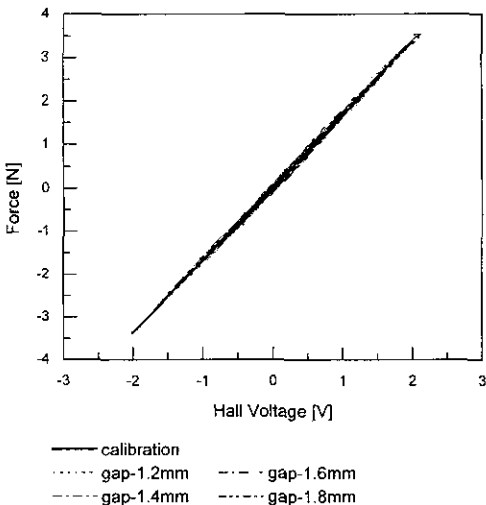


Fig. 7 Force calibration of Hall sensor: harmonic test

neously. Figure 7 shows the typical calibration curves with air gap varied. The calibration results are summarized in Table 1. Note that the Hall sensor has a relatively wide frequency bandwidth

Table 1 Calibration results (dynamic characteristics)

Calibration factor		1.685	
Resolution	0.04 N	Sensitivity	590 mV/N
Linearity (0~5N)	*61.5 %	Range	0~7N
Bandwidth (-3dB)	830 Hz	Supply Current	7 mA

and good accuracy.

5. Experiments

5.1 Experimental set-up

Figure 8 shows the schematic of an experimental set-up for the complex modal testing of a flexible rotor bearing system. The test rotor (Bently Nevada rotor kit: Model 24755) consists of a shaft, two ball bearings and two rigid disks. A motor with the tacho feedback feature drives the rotor system through a flexible coupling. A pair of magnetic exciters, driven by two independent random signals from the noise generators (B&K Model 1027), excites the rotor for the standard two-exciter method. For the one-exciter method, a uni-directional excitation force is applied to the rotor system. The resulting excitation forces are measured by Hall sensors (SIEMENS, KSY44) and the responses in the y- and z-directions are measured using a pair of eddy-current type proximity probes. The measured force and response signals are filtered using anti-aliasing analog filters (WAVETEC Model 852) with a nominal cut-off frequency of 200Hz and sampled at a rate of 450Hz by a data acquisition board (National Instrument Model AT-MIO-16E-10). Each data set consists of 2048 data points that are averaged up to 200 times. An encoder is used to measure the rotational angle and speed, when the test rotor is operated at 600 rpm (10Hz).

5.2 Modal testing of asymmetric rotors

To demonstrate the modal testing method for a rotor with shaft asymmetry, an artificial local slot was made on the shaft with the radius of 9.5 mm

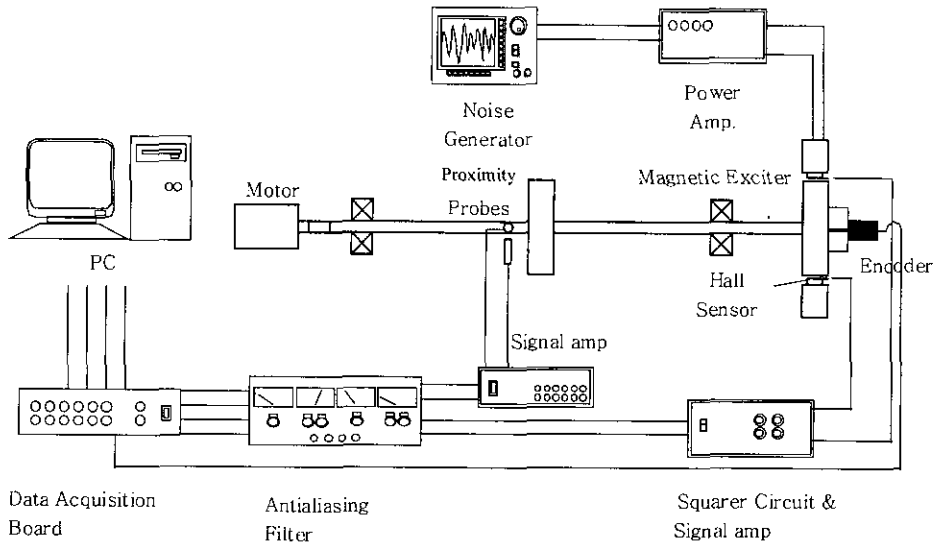


Fig. 8 Experimental set-up for modal testing of rotor

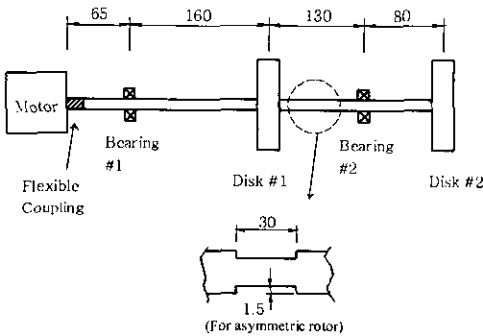


Fig. 9 Rotor with shaft asymmetry

as shown in Fig. 9. Two identical disks with the mass of 0.9 kg and polar and diametric moments of inertia of 0.0006kgm² and 0.0003kgm², respectively, are mounted on the shaft.

Since the differential equations of motion for asymmetric rotors, when written with respect to the stationary coordinate system, essentially are characterized by the presence of time varying coefficients, the modulation of measured signals is needed to estimate the dFRFs, requiring precise measurement of the rotational angle (Δt) and speed. For this purpose, an encoder is attached at the free end of the shaft through a flexible coupling. The dFRFs, especially the reverse dFRF, are very sensitive to any mismatch of rotational angles. Hence, the rotational angles must be precisely measured and carefully calibrated. Dur-

ing the test, the overhung disk #2 is excited in both y and z directions using the magnetic exciter with two independent band limited random noises (0-300Hz). The resulting rotor responses are measured near disk #1 using a pair of proximity probes.

The dFRFs for the asymmetric rotor can be obtained as shown in Fig. 10 using the standard two-exciter/two-sensor method. Figure 10 shows that the first backward (1B[-47Hz]) and forward (marked 1F[47Hz]) modes are well separated in the normal dFRF. The first conjugate modes (marked 1B̄[-28Hz] and 1F̄[66Hz]) also appear clearly in the normal dFRF. The second backward (2B[-116Hz]) and forward (2F[116Hz]) modes are also clearly identified in the normal dFRF. However, the second conjugate modes (2B̄[-81Hz], 2F̄[134Hz]) do not appear clearly in the normal dFRF. The conjugate modes of the asymmetric rotor appear to be almost symmetrical with respect to the rotational frequency (10Hz), in contrast to the zero frequency for the anisotropic rotor systems. The second modes in the reverse dFRF cannot be clearly identified due to the presence of the noise. However, the second modes are also symmetric with respect to the rotational frequency axis. The phase at 85Hz indicates that the peak near 85Hz is not a mode, and may be caused by weak

anisotropy of the rotor (Joh and Lee, 1996).

5.3 Comparison of complex modal testing methods

The estimated dFRFs obtained from two differ-

ent methods, described in Sec. 3, are compared in Fig. 11. For the one-exciter/two-sensor method, the normal and reverse dFRFs shown in Fig. 11 (a) are almost the same as the two-exciter/two-sensor method. For the two-exciter/ one-sensor

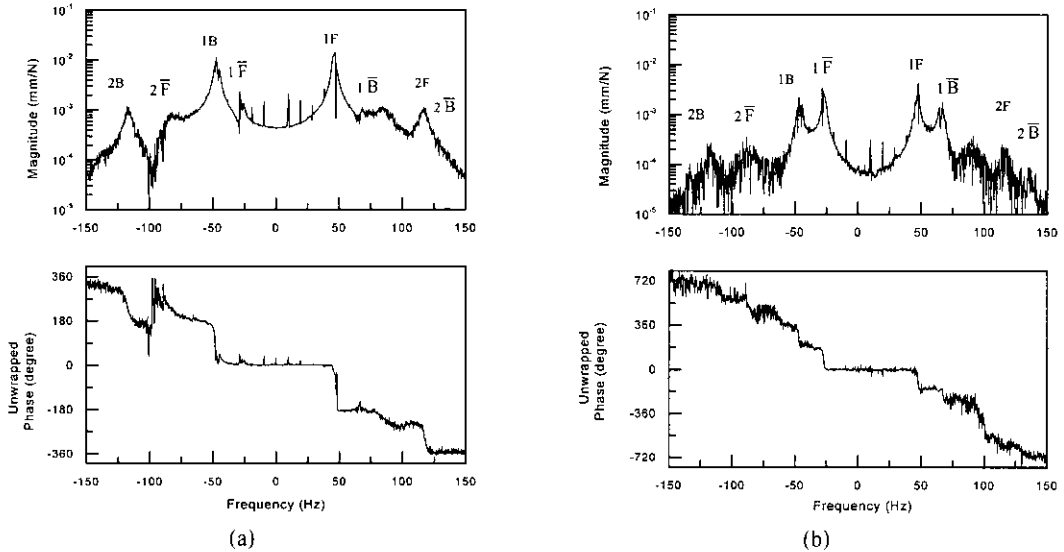


Fig. 10 Magnitude-phase plots of (a) $H_{gp}(j\omega)$ and (b) $H_{gp}(j\omega)$: at $\Omega=600$ rpm (10Hz) using 2X-2S method

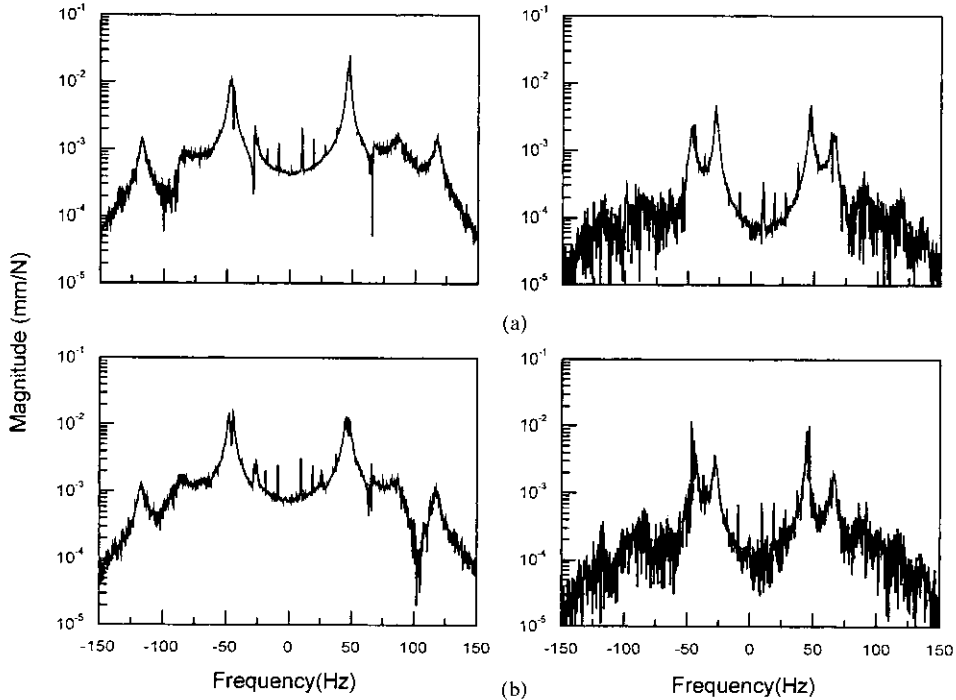


Fig. 11 Magnitude plots of $H_{gp}(j\omega)$ and $H_{gp}(j\omega)$: (a) 1X-2S method (b) 2X-1S method

Table 2 Summary of excitation and measurement techniques

MODAL TESTING METHOD	REMARK
two-exciter/two-sensor method	a pair of uncorrelated random input signals with equal power
one-exciter/two-sensor method	the most effective method
two-exciter/one-sensor method	sensitive to anisotropy and noise

method, the normal dFRF shown in Fig. 11 (b) is nearly the same as that using the two-exciter/ two-sensor method, except for the splitting of the first modal peak into two distinct peaks. The result implies that the two-exciter/one-sensor method is rather sensitive to the system anisotropy (stator asymmetry). The reverse dFRF is affected by the noise to a much greater extent than in the two-exciter/two-sensor method and the one-exciter/ two-sensor method.

As a result, the noise affects the reverse dFRF significantly as the number of sensors is reduced to just one (i. e. the two-exciter/one-sensor method). The experimental results indicate that the one-exciter/two-sensor method is the most effective method, considering the quality of the results and implementation practicality. The one-exciter/two-sensor method greatly lessens the testing effort compared with the bi-directional excitation method. The comparison of the methods is summarized in Table 2.

6. Conclusions

A magnetic exciter equipped with Hall sensors is developed and successfully used for the complex modal testing of a rotor. The test system is inexpensive, easy to move and convenient to install/assemble. The force calibration experiments also show that Hall sensors can measure the magnetic excitation force with a wide bandwidth and a good resolution. The complex modal experiments using the laboratory test rotor with an open crack were carried out in order to

evaluate the performance of the various testing methods. It is found that, among others, the one-exciter/two-sensor method is the most effective in terms of practical implementation and the measurement accuracy in estimating the dFRFs associated with the asymmetric rotors.

Acknowledgments

This work has been supported by the Critical Technology 21 Project from the Ministry of Science and Technology, Korea and a grant by the Agency of Defense Development, Korea.

References

- Jei, Y. G. and Lee, C. W., 1988, "Finite Element Model of Asymmetrical Rotor Bearing Systems," *KSME Journal*, Vol. 2, No. 2, pp. 116 ~124.
- Lee, C. W., 1991, "A Complex Modal Testing Theory for Rotating Machinery," *Mechanical Systems and Signal Processing*, Vol. 5, No. 2, pp. 119~137.
- Lee, C. W., 1993, *Vibration Analysis of Rotors*, Kluwer Academic Publishers.
- Lee, C. W. and Kim, J. S., 1992, "Modal Testing and Suboptimal Vibration Control of Flexible Rotor Bearing System by Using a Magnetic Bearing," *ASME J. Dynamic Systems, Measurement and Control*, Vol. 114, pp. 244 ~252.
- Gähler, C. and Forch, P., 1994, "A Precise Magnetic Bearing Exciter for Rotordynamic Experiments," *4th Int. Symposium on Magnetic Bearing*, Zurich, Switzerland.
- Joh, C. Y. and Lee, C. W., 1996, "Use of dFRFs for Diagnosis of Asymmetric/Anisotropic Properties in Rotor-Bearing System," *ASME J. Vibration and Acoustics*, Vol. 118, No. 1, pp. 64 ~69.
- Lee, C. W. and Lee, S. K., 1997, "An Efficient Complex Modal Testing Theory for Asymmetric Rotor Systems: Use of Unidirectional Excitation Method," *Journal of Sound and Vibration*, Vol. 206, No. 3, pp. 327~338.
- Lee, C. W. and Kwon, K. S., 1999, "Identifica-

tion of Rotating Asymmetry in Rotating Machines by Using Reverse dFRF,” *ASME, Design Technical Conference*, Las Vegas, DETC99/VIB-8267.

Bendat, J. S. and Piersol, A. G., 1986, *Random Data: Analysis and Measurement Procedures*,

John Wiley & Sons.

Lee, C. W., Yoon, Y. K. and Jeong, H. S., 1997, “Compensation of Tool Axis Misalignment in Active Magnetic Bearing Spindle System,” *KSME International Journal*, Vol. 11, No. 2, pp. 155~163.